Cell Stem Cell
Article

CD44v6 Is a Marker of Constitutive and Reprogrammed Cancer Stem Cells Driving Colon Cancer Metastasis

Matilde Todaro,[1,5] Miriam Gaggianesi,[1] Veronica Catalano,[1,5] Antonina Benfante,[1,5] Flora Iovino,[1] Mauro Biffoni,[2] Tiziana Apuzzo,[1,5] Isabella Sperduti,[3] Silvia Volpe,[1] Gianfranco Cocorullo,[1] Gaspare Gulotta,[1] Francesco Dieli,[4,5] Ruggero De Maria,[3,*] and Giorgio Stassi[1,*]

[1]Surgical and Oncological Sciences, University of Palermo, 90127 Palermo, Italy
[2]Department of Hematology and Oncology, Istituto Superiore di Sanità, 00161 Rome, Italy
[3]Regina Elena National Cancer Institute, 00144 Rome, Italy
[4]Biopathology and Biomedical Methodologies, University of Palermo, 90134 Palermo, Italy
[5]Central Laboratory of Advanced Diagnosis and Biomedical Research (CLADIBIOR), University of Palermo, 90127 Palermo, Italy
*Correspondence: demaria@ifo.it (R.D.M.), giorgio.stassi@unipa.it (G.S.)
http://dx.doi.org/10.1016/j.stem.2014.01.009

SUMMARY

Cancer stem cells drive tumor formation and metastasis, but how they acquire metastatic traits is not well understood. Here, we show that all colorectal cancer stem cells (CR-CSCs) express CD44v6, which is required for their migration and generation of metastatic tumors. CD44v6 expression is low in primary tumors but demarcated clonogenic CR-CSC populations. Cytokines hepatocyte growth factor (HGF), osteopontin (OPN), and stromal-derived factor 1α (SDF-1), secreted from tumor associated cells, increase CD44v6 expression in CR-CSCs by activating the Wnt/β-catenin pathway, which promotes migration and metastasis. CD44v6^{-} progenitor cells do not give rise to metastatic lesions but, when treated with cytokines, acquire CD44v6 expression and metastatic capacity. Importantly, phosphatidylinositol 3-kinase (PI3K) inhibition selectively killed CD44v6 CR-CSCs and reduced metastatic growth. In patient cohorts, low levels of CD44v6 predict increased probability of survival. Thus, the metastatic process in colorectal cancer is initiated by CSCs through the expression of CD44v6, which is both a functional biomarker and therapeutic target.

INTRODUCTION

Due to the extreme difficulties to cure distant metastasis, colorectal cancer (CRC) is the second leading cause of cancer death in Western countries (Jemal et al., 2011). The complex mechanisms leading to cancer metastasis are far from being completely understood, and it is still unclear which cell subset is able to migrate, survive, and grow at the metastatic site (Chaffer and Weinberg, 2011).

In recent years, a growing body of evidence has provided support for the existence of cellular hierarchies within many tumor types where cancer stem cells (CSCs), commonly identified by their cell-surface-marker expression, are the unique source of all tumor cells and responsible for tumor propagation and relapse (Valent et al., 2012). CSCs, defined by their capacity for self-renewal and resistance to conventional chemotherapies, are believed to remain after cancer therapy to initiate the metastatic process (Brabletz et al., 2005), and their ability to do so has been reported for several forms of cancers. Human pancreatic CSCs expressing the putative stem cell marker CD133 and the chemokine receptor CXCR4 lost their metastatic activity when the CXCR4^{+} population was depleted, suggesting that CSCs may hijack cytokine-regulated migration-signaling pathways to initiate metastasis (Hermann et al., 2007). In breast cancer, ectopic expression of Twist and Snail, two transcription factors directly involved in epithelial mesenchymal transition (EMT) and metastasis development, lead to increased expression of stem cells markers and enhanced tumorigenesis, indicating that a tight connection between EMT activation and CSC phenotype drives the metastatic process (Mani et al., 2008). More recently, a CD26^{+} CSC population present in both primary colorectal tumors and liver metastasis was demonstrated to give rise to metastatic lesions in the liver when orthotopically injected in immunocompromised mice (Pang et al., 2010). These studies provide a few examples of cancers where CSCs isolated from both primary and metastatic tumors were demonstrated to have the capacity to initiate metastasis. However, whether the cell-surface markers that identify CSCs play a functional role in the molecular events within the tumor environment that drive tumorigenesis and result in the cancer spreading to other organs has been difficult to pinpoint for most CSC populations identified to date. This is an important goal for the field, because understanding whether the cell-surface phenotype of CSC is mechanistically linked with the metastatic process may help develop effective therapeutic agents targeting CSCs.

CD44 is a widely expressed polymorphic integral membrane adhesion molecule that binds hyaluronic acid and contributes to cell-cell and cell-matrix adhesion, cell growth and trafficking, EMT, and tumor progression (Orian-Rousseau, 2010). The vast majority of tumors express CD44, whose detection in combination with other antigens is able to enrich for CSCs in several different tumor types (Al-Hajj et al., 2003; Dalerba et al., 2007; Lee et al., 2008; Patrawala et al., 2006; Pries et al., 2008; Zhang

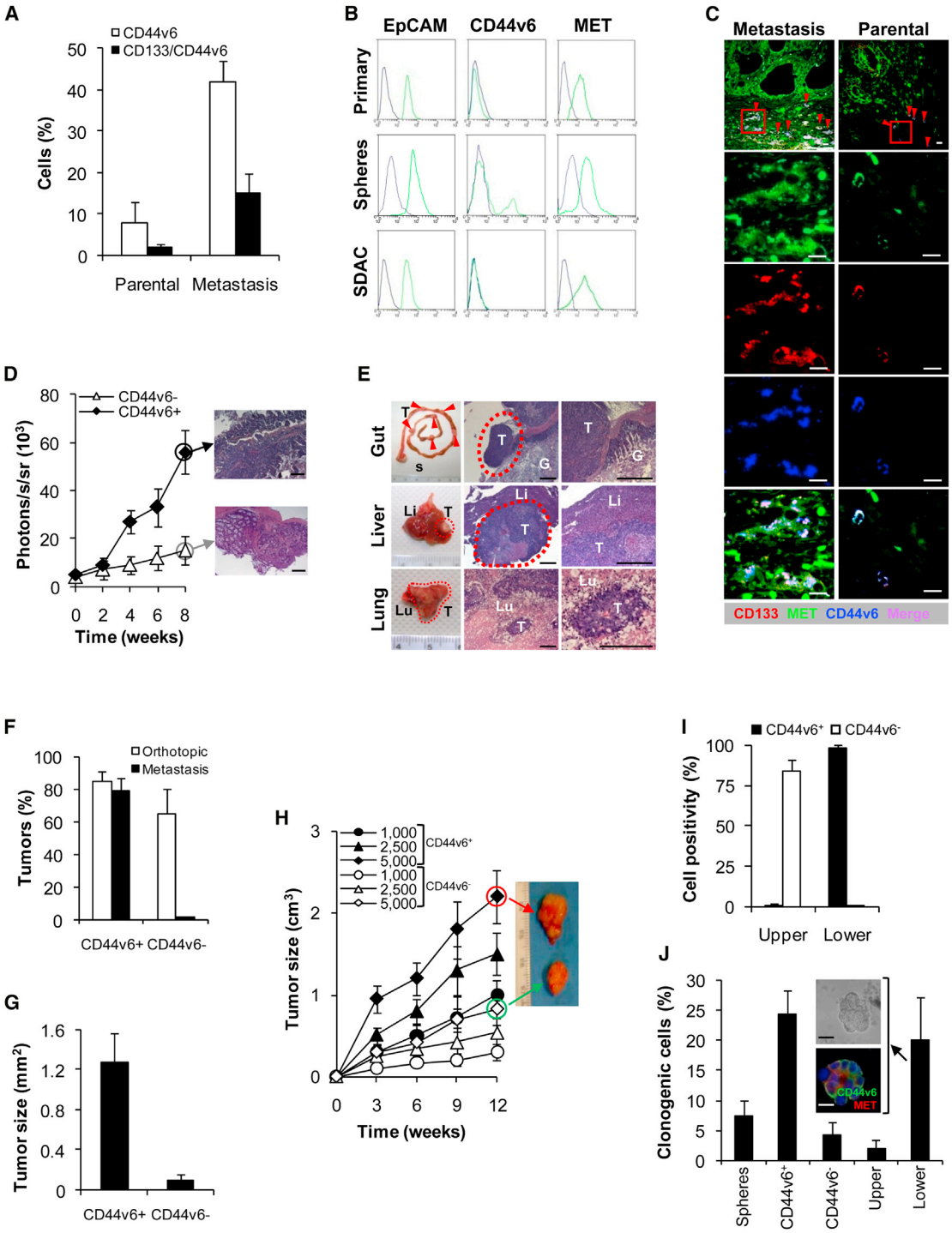

Figure 1. Metastatic CRC Cells Express CD44v6

(A) Percentage of CD44v6 and CD133 on gated EpCAM$^+$ cells assessed by flow cytometry on freshly purified CRC cells from parental tumor and corresponding liver metastasis. Data are mean ± SD from independent experiments performed with cells from ten different patients.

(B) Flow cytometry profiles of EpCAM, CD44v6, and MET on primary, spheres, and SDAC.

(C) Immunofluorescence analysis of CD133, MET, and CD44v6 on paraffin-embedded sections of parental CRC and its liver metastasis tissue at the front of invasion. Red arrowheads indicate tumor buds expressing CD133/MET/CD44v6. One representative experiment of 12, performed with tissues derived from different patients, is shown. The scale bars represent 20 μm.

(D) Kinetics of in vivo whole-body imaging analysis of orthotopic tumor growth and metastasis formation following injection of 5 × 10^3 CD44v6$^+$ or CD44v6$^-$ cells. Data are mean ± SD of four independent sets from different donors of six tumors per group. Right, hematoxylin and eosin (H&E) staining of mouse caecum bearing primary tumors generated by injection of CD44v6$^+$ and CD44v6$^-$ cells. The scale bars represent 150 μm.

(legend continued on next page)

et al., 2008). *CD44* transcripts undergo complex alternative splicing, resulting in functionally different isoforms expressed primarily on epithelial cells (Tölg et al., 1993). Although the expression of standard isoform (CD44s) has been more extensively studied, the variant isoforms (CD44v) seem restricted to subpopulations endowed with stem cell potential and cancer development. This seems to be particularly true in the gut. Although intestinal stem cells express both standard and variant CD44 isoforms, CD44v, but not CD44s, isoforms promote the generation of gut adenoma in mouse models of familial adenomatous polyposis (Zeilstra et al., 2014). Among CD44v isoforms, CD44v6 seems to play a major role in cancer progression for its ability to bind hepatocyte growth factor (HGF), osteopontin (OPN), and other major cytokines produced by tumor microenvironment (Orian-Rousseau, 2010). The major role of CD44v6 involves cell migration and invasion. CD44v6 interacts with hepatocyte growth factor receptor (MET) in the presence of HGF and potentiates its signaling (Orian-Rousseau et al., 2002). CD44v expression is downstream of the Wnt signaling and induced by the β-catenin/Tcf-4 signaling pathway (Wielenga et al., 2000). Nuclear β-catenin accumulates in the undifferentiated CRC cells at the invasive front, whereas a gradual loss is detected in the well-differentiated tumor areas, suggesting its role as marker predictor for cancer metastasis (Brabletz et al., 2005).

The interaction between tumor and its microenvironment is critical for cancer progression, which is promoted by different cytokines produced by stroma or accessory cells present in proximity to the tumor lesion (Whiteside, 2008). OPN is a cytokine produced by fibroblasts and immune and endothelial cells that is involved in several biological processes during bone turnover, tumorigenesis (Rangaswami et al., 2006), inflammation, and immune response (Cantor and Shinohara, 2009). In CRC, elevated CXCR4 expression correlated with advanced tumor stages III/IV and may help identify patients with higher probability to metastasize to the liver (Schimanski et al., 2005). Likewise, the functional expression of MET and HGF has been shown to provide a selective growth advantage to neoplastic cells at different stages of tumor progression (Di Renzo et al., 1995).

Here, we investigated whether mechanisms regulating CD44 isoforms during developmental process would be mirrored by colorectal (CR)-CSCs during tumorigenesis and metastatic spread. We show that CR-CSCs are included in the CD44v6$^+$ population and that such CD44v6 expression confers metastatic potential to all CR-CSCs. Engagement of MET and its coreceptor CD44v6 in CR-CSCs activates an EMT program that promotes cell motility, invasiveness, and metastasis. Furthermore, we demonstrated that HGF, OPN, and stromal-derived factor 1α (SDF-1) induce CD44v6 expression in CRC progenitor cells, which increase the tumorigenic activity while acquiring the ability to produce metastasis. Our data indicate CD44v6 as a molecule that could be clinically exploited both as a biomarker and therapeutic target in CRC.

RESULTS

CD44v6 Expression Demarcates a Highly Tumorigenic CR-CSC Population with Metastatic Potential

We and others previously demonstrated that CR-CSCs are enriched in tumor spheres or freshly isolated CD133$^+$ cells (O'Brien et al., 2007; Ricci-Vitiani et al., 2007; Todaro et al., 2007). Given that CD44 has been reported as a CR-CSC marker (Dalerba et al., 2007), we set out to investigate whether expression of CD44 variants might stratify CR-CSCs into subpopulations with distinct functional properties. Although several of the variable *CD44* exons were uniformly translated across patient-derived CRC subsets, mRNA levels of *CD44v5* and *CD44v6* appeared considerably higher in sphere-propagated CSCs and in freshly purified CD133$^+$cells relative to sphere-derived differentiated progeny and bulk primary cells (Figure S1A available online). Analysis of *CD44v5* mRNA in CD44v6$^+$ cells purified from patient tumors or spheres further suggested that *CD44v5* and *CD44v6* are translated in the same subset of CRC cells (Figure S1B). Interestingly, CD44v6 is significantly higher expressed in metastatic lesions than in their corresponding primary tumors (Figure 1A). In contrast, we found that CD44$^+$-expressing cells were equally present across CRC sphere cells and differentiated progeny and in primary and metastatic tumors (Figure S1C).

Although MET, which is known to interact with CD44v6, was prominently expressed in both primary and metastatic CRCs (Figure S1D), subsets of CRC cells enriched in stem-like cells, such as CD133$^+$, CD166$^+$, Lgr5$^+$, EphB2^{bright}, and tumor spheres, all contain a small but consistently present CD44v6$^+$ population (Figures 1B, S1E, and S1F). Intriguingly, immunofluorescence analysis of tumor sections indicated that CD44v6$^+$ cells were mainly located as tumor buds at the invasion front of aggressive tumors and largely express CD133 (Figure 1C).

(E) Macroscopic analysis (left) and H&E staining (central panels) with corresponding magnifications (right) of tumors grown in the gut, liver, and lung after orthotopic injection of CD44v6$^+$ cells. Stomach (S), gut (G), liver (Li), lung (Lu), and tumors (T) are indicated. Red arrowheads highlight tumor multifocal dissemination along the gut. Dotted circles emphasize metastatic foci. The scale bars represent 200 μm.

(F) Percentage of colon tumor and liver metastasis growth after 12 weeks in mice orthotopically injected with freshly purified CD44v6$^+$ and CD44v6$^-$ populations. Data are mean ± SD of results obtained from 18 independent experiments performed with cells of six different patients.

(G) Tumor size measured on sections stained for H&E of orthotopic growth following injection of freshly purified parental cancer cells enriched in CD44v6$^+$ and CD44v6$^-$ populations. Samples were analyzed 16 weeks after cell injection. Data are mean ± SD of the analysis of 21 tumor xenografts using cells purified from seven different CRC patients.

(H) Size of subcutaneous tumors following injection of 1,000, 2,500, and 5,000 CD44v6$^+$ and CD44v6$^-$ cells magnetically sorted from CRC spheres. Right, one representative gross morphology of tumor xenografts grown for 12 weeks and generated by the injection of 5,000 cells. Data are mean tumor size ± SD of four tumors per group derived from three separate patients.

(I) Percentage of CD44v6$^+$ and CD44v6$^-$ sphere cells collected from the upper (upper) and lower (lower) layers of transwell chamber, in presence of conditioned medium from NIH 3T3 cells (NIH 3T3-CM), detected by flow cytometry.

(J) Clonogenic assay of spheres, CD44v6$^+$- and CD44v6$^-$-enriched sphere cells, and cells harvested as in (I). Data are expressed as mean ± SD of six independent experiments, performed with cells from different patients. (Inset) Representative phase contrast image and immunofluorescence analysis for CD44v6 (green color) and MET (red color) on spheres grown in the lower part of transwell. The scale bars represent 20 μm.

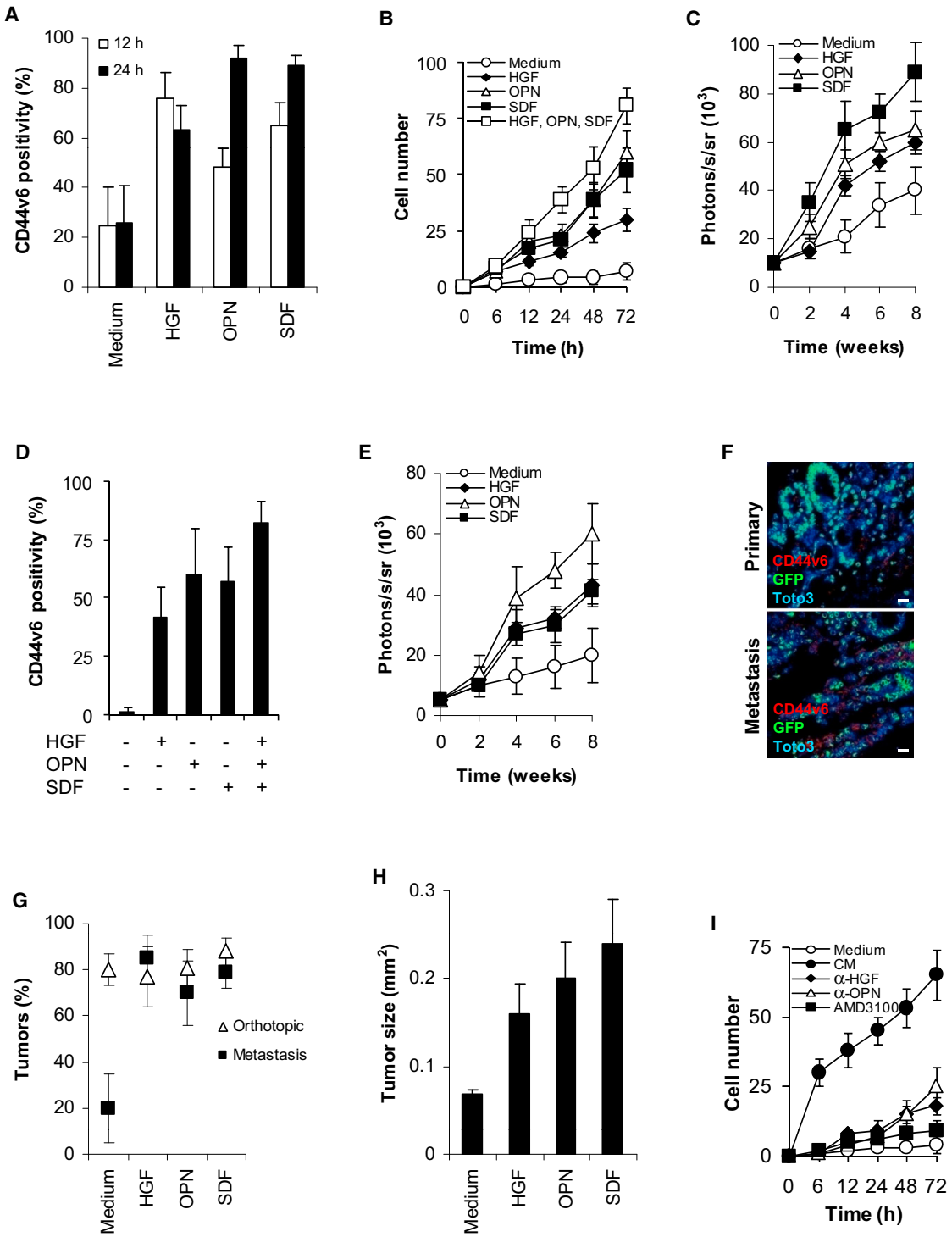

Figure 2. HGF, OPN, and SDF-1 Increase the Number of CD44v6 Cells Sustaining the Metastatic Activity of CR-CSCs

(A) Percentage of CD44v6$^+$ cells by flow cytometry in untreated and treated sphere cells with HGF, OPN, and SDF at the indicated time. Data are expressed as mean ± SD of six independent experiments.

(B) Invasion assay of sphere cells using stem cell medium (SCM; medium) in presence of HGF, OPN, SDF alone, or in combination. Data are mean ± SD of five independent experiments performed using cells from different patients.

(C) In vivo imaging analysis of tumor and metastasis outgrowth at the indicated time points. Xenografts were generated by using CRC sphere cells implanted orthotopically and pretreated for 24 hr as in (A). Data are mean ± SD of four independent experiments using cells from different patients.

(D) Induction of CD44v6 expression in CD44v6$^-$ sphere cells untreated and stimulated with HGF, OPN, and SDF, alone or in combination for 24 hr by flow cytometry.

(legend continued on next page)

Both CD44v6$^+$ and CD44v6$^-$ CRC sphere cells displayed tumorigenic potential in vivo. However, CD44v6$^-$ cells generated only small orthotopic tumors, whereas the CD44v6$^+$ cell fraction robustly generated metastatic lesions in the gut, liver, and lung (Figures 1D, 1E, S2A, and S2B). Likewise, whereas freshly isolated CD44v6$^+$ cells were able to generate both orthotopic tumors and metastasis, their negative counterparts grew locally as small tumors, without forming distant lesions (Figures 1F–1H, and S2C). The tumorigenic capacity of the CD44v6$^-$ population was entirely lost in secondary recipients, suggesting that CD44v6$^-$ cells include transient amplifying progenitors and more differentiated nontumorigenic cells whereas metastatic CR-CSCs are confined to the small CD44v6$^+$ population (Figure S2D).

CD26 has been reported as a marker of invasive and metastatic CR-CSCs (Pang et al., 2010). Although more than 50% of the CD44v6$^+$/MET$^+$/CD133$^+$ cells express CD26 (Figure S2E), CD44v6$^+$/CD26$^-$ CR-CSCs showed considerable metastatic potential in the orthotopic model (Figure S2F), indicating that CD26 expression is not informative for metastatic activity of the CD44v6 population.

To analyze the CD44v6$^+$ and CD44v6$^-$ cells in more detail, we investigated their invasive and clonogenic potential. In vitro migration analysis confirmed that the invasion capability resided entirely in the CD44v6$^+$subset (Figure 1I), in which *Twist* and *Snail* are translated (Figure S2G). Invading CRC cells also showed MET phosphorylation, nuclear accumulation of β-catenin, complete loss of E-cadherin, and acquisition of vimentin expression (Figures S2H–S2J). Moreover, limiting dilution analysis showed that the clonogenic activity of CD44v6$^+$ and migrating cells was significantly increased relative to bulk sphere cells, whereas CD44v6$^-$ and nonmigrating cells were poorly clonogenic (Figure 1J).

HGF, OPN, and SDF-1 Regulate CD44v6 Expression and Drive the Metastatic Process

We next evaluated whether cytokines known to promote cancer cell migration would affect tumorigenic properties and levels of CD44v6 expression in CD44v6$^-$ CRC populations. In CRC sphere cells, exposure to HGF, OPN, and SDF-1 promoted the expression of CD44v6 with a minimal induction of *CD44v5*, while concomitantly enhancing cell migration and metastatic activity without altering MET expression (Figures 2A–2C and S3A–S3C). Likewise, in the presence of these cytokines, CD44v6$^-$ progenitor cells acquired CD44v6 expression and gained in vivo metastatic potential together with a more aggressive phenotype (Figures 2D–2F and S3D). Consequently, freshly isolated primary CRC samples formed distant lesions, which appeared as micrometastasis 3 months after injection only from cells that had been exposed to HGF, OPN, or SDF-1 (Figures 2G, 2H, and S3E). However, when primary CRC cells from CD44v6$^-$ samples were exposed to HGF, OPN, or SDF-1 (Figure S3F), CD44v6 expression remained low in the vast majority of cells, suggesting that only transiently amplified CD44v6$^-$ progenitors can be converted to CD44v6$^+$ cells. Whereas HGF binds to CD44v6 and MET, SDF-1 binds to CXCR4, which is expressed by both CD44v6$^-$ and CD44v6$^+$ in parental and CRC sphere cells (Figure S3G). We found that blocking SDF-1 activity with the CXCR4 antagonist AMD3100 in sphere cells reduced their invasive capability (Figure 2I). Interestingly, SDF-1 blockage also abrogated the upregulation of CD44v6 induced by HGF and OPN (Figure S3H). Because both HGF and OPN are known to upregulate CXCR4 and SDF-1, it is likely that both HGF and OPN act via the CXCR4/SDF-1 axis in CD44v6$^-$ cells.

Cancer-Associated Fibroblasts Promote the Tumorigenic and Metastatic Activity of CRC Stem and Progenitor Cells

Cancer-associated fibroblasts (CAFs) are key players in the tumor microenvironment known to secrete compounds that potentiate tumor malignancy (Hanahan and Coussens, 2012). Conditioned medium from CAFs (CAF-CM) increased the clonogenic activity of sphere-cultured CRC cells, enhanced the migration of CD44v6$^+$ cells, and turned nonmigrating CD44v6$^-$ cells into migrating CD44v6$^+$ cells, demonstrating that CAFs secrete compounds that increase self-renewal and invasion potential of CRC cells (Figures 3A and 3B). Both constitutive and cytokine-induced CD44v6 expression was significantly reduced in CRC spheres treated with fetal bovine serum (FBS) (Figures 3C and S4A), suggesting that the absence of serum allows CAF-CM to promote the expression of CD44v6 in undifferentiated CRC cells. Whereas short-term exposure to CAF-CM or cytokines resulted in a transient induction of CD44v6 in CD44v6$^-$ sphere cells, a prolonged stimulation maintained CD44v6 expression for several weeks, so that cells became functionally similar to CD44v6$^+$ cells (Figures S4B and S4C).

We found that both CD44v6$^+$ and CD44v6$^-$ CRC sphere cells, when treated with CAF-CM or cotransplanted subcutaneously with CAFs, gave rise to larger primary and secondary tumors (Figures 3D, 3E, and S4D). Immunohistochemical analysis revealed that HGF, OPN, and SDF-1 could only be detected in xenografts formed by CD44v6$^-$ cells coinjected with CAFs (Figure S4E), suggesting that these compounds are secreted by CAFs during CRC tumorigenesis. Accordingly, primary cultured CAFs and freshly isolated CD90$^+$ cells from tumor specimens produced significantly higher levels of HGF, OPN, SDF-1, and

(E) In vivo imaging analysis of tumor and metastasis growth at the indicated time points. Xenografts were generated using CD44v6$^-$ sphere cells pretreated for 24 hr as in (D).

(F) Immunofluorescence analysis of GFP and CD44v6 on paraffin-embedded sections of primary tumor xenograft (primary) and its lung metastasis (metastasis) derived by the orthotopic injection of CD44v6$^-$ cells transduced with LUC-GFP and treated with HGF. The scale bars represent 20 μm.

(G) Frequency of primary tumor and metastasis formation after 12 weeks in immunodeficient mice injected with freshly purified parental CRC cells, untreated and pretreated for 24 hr with HGF, OPN, and SDF.

(H) Tumor size evaluated on paraffin-embedded sections of CRC xenografts generated by orthotopic injection of freshly purified parental cancer cells treated as in (G). Data are mean ± SD of 21 tumor xenografts generated by freshly purified cancer cells from seven different patients.

(I) Invasion assay performed with NIH 3T3-CM (CM) up to 72 hr of sphere cells untreated and treated with α-HGF, α-OPN, or AMD3100. Data are mean ± SD of five independent experiments performed using cells from different patients.

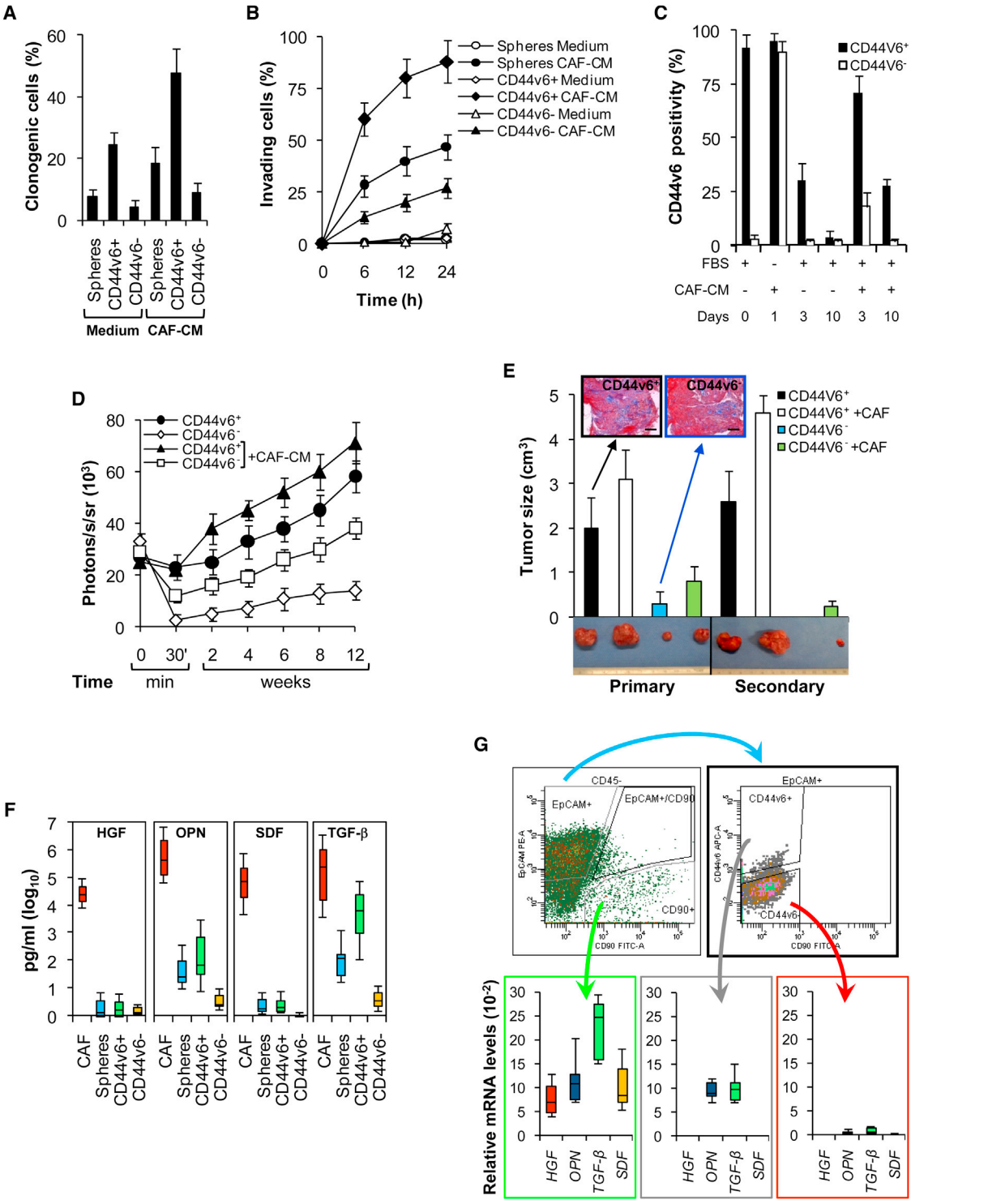

Figure 3. CAFs Improve the Metastatic Potential of CRC Cells

(A) Clonogenic assay of spheres and CD44v6$^+$- and CD44v6$^-$-enriched cells cultured in presence of SCM (medium) or conditioned medium from cancer-associated fibroblasts (CAF-CM).

(B) Invasion assay of sphere cells (spheres) and CD44v6$^+$- and CD44v6$^-$-enriched sphere cell populations cultured as in (A). Data are mean ± SD of five independent experiments using cells from different patients.

(C) Flow cytometry analysis of CD44v6 in CD44v6$^+$ and CD44v6$^-$ sphere cells untreated and treated with 10% FBS or CAF-CM at the indicated time points. Data are expressed as mean ± SD of four independent experiments.

(legend continued on next page)

transforming growth factor β (TGF-β) than sphere-cultured CRC subsets (Figures 3F and 3G).

CD44v6 and MET Are Required for CRC Metastasis

To confirm that CD44v6 is required for migration of tumorigenic cells, we compared the inhibitory effect of CD44v6, HGF, or MET targeting on CR-CSCs. Transduction of spheres with lentiviral vectors encoding for specific *CD44v6* and *MET* small hairpin RNA (shRNA) sequences significantly reduced their mRNA and protein levels, respectively (Figures S5A, S5B, and S5C), while abolishing cell migration (Figure 4A). A similar inhibitory effect was obtained using a blocking CD44v6 antibody or shCD44v6, whereas HGF neutralization was slightly less effective (Figure 4A).

We next investigated whether *MET* silencing in CD44v6$^+$ CSCs could have in vivo therapeutic benefits. Purified and depleted CD44v6 cells from CRC spheres transduced with shCD44v6 or inducible shMET were allowed to orthotopically grow into the mouse caecum. MET and CD44v6 knockdown abrogated tumor metastasis outgrowth, indicating that CSCs need both molecules for tumor spreading (Figures 4B, 4C, and S5D), whereas exogenous expression of CD44v6 restored the migration of CD44v6$^-$ cells (Figures 4D, S5E, and S5F). To determine whether CD44v6 is required for the metastatic activity of CRC cells in a syngeneic model, enriched and depleted CD44v6 cells from the mouse colon-26 line were implanted into BALB/c mice spleens and analyzed for their migration ability. Again, CD44v6$^-$ cells were unable to colonize the liver, whereas CD44v6$^+$ cells were readily detected into the liver 30 min after spleen injection (Figures 4E and S5G). Of note, exposure to neutralizing antibody against CD44v6 was able to prevent tumor spreading sustained by freshly isolated cells without affecting the orthotopic engraftment (Figure 4F), indicating that CD44v6 may act as a functional marker of cells with metastatic potential in CRC. Because CD44v6 and CD44v5 are coexpressed (Figures 4G, S1A, and S1B), we evaluate the involvement of CD44v5 in the metastatic activity of CR-CSCs. Exogenous expression of CD44v5 in CD44v5$^-$/CD44v6$^-$ CRC sphere cells promoted the expression of CD44v6 (Figures S5H and S5I), allowing the cells to become metastatic in the spleen-liver assay (Figure 4H). Altogether, these results suggest that CD44v6 could be a promising therapeutic target to prevent metastasis formation in CRC.

Wnt and BMP Pathways Control CD44v6 Expression and CSC Activity

The activation of the Wnt/β-catenin pathway is the hallmark of CR-CSCs. CD133$^+$ CRC cells expanded in culture as tumor spheres contain a subset of tumorigenic cells with constitutively high Wnt signaling, which can be detected by a β-catenin/GFP reporter (Vermeulen et al., 2010). By flow cytometry analysis, we also found that the vast majority of CD44v6$^+$ cells in CRC spheres display high β-catenin activity (Figure 5A), in line with the high tumorigenic activity of these cells. Interestingly, immunofluorescence analysis of tumor sections indicated that CD44v6$^+$ cells at the invasion front of aggressive tumors largely express nuclear β-catenin (Figure 5B). Of note, Wnt3a was able to increase expression levels of CD44v6 and clonogenic and migration activity of CRC stem and progenitor cells (Figures 5C–5E). Moreover, the analysis of CD44v6$^-$ transduced with CD44v5 showed that the acquisition of CD44v6 paralleled the activation of β-catenin (Figure 5F), confirming the prominent role of the Wnt signaling pathway in this system. In accordance with the functional differences observed in CD44v6$^+$ and CD44v6$^-$ cells, cytokines able to upregulate CD44v6 promoted the expression of Wnt-, EMT-, and metastasis-related genes (Figure 5G). Each of these cytokines was able to activate the β-catenin pathway in CRC spheres (Figure 5H), in line with their ability to promote a prometastatic phenotype in CD44v6$^-$ CRC sphere cells.

Bone morphogenetic protein 4 (BMP4) and BMP2 are produced by differentiated CRC cells and are absent in cancer stem and progenitor cells (Hardwick et al., 2004; Lombardo et al., 2011). Because BMP4 promotes the differentiation of CR-CSCs and antagonizes the Wnt pathway, we hypothesized that BMPs could repress the expression of CD44v6. CD44v6$^+$ cells gradually decreased their β-catenin activity in presence of BMP4 (Figure 5I). Cytokine- and CAF-CM-induced CD44v6 expression was significantly reduced in CRC spheres treated with BMP2 or BMP4 (Figure 5J), suggesting that the absence of differentiating agents allows HGF, OPN, and SDF-1 to promote the expression of CD44v6 in undifferentiated CRC cells. Thus, the ability of BMPs to promote the differentiation and loss of tumorigenic activity of CR-CSCs is paralleled by the repression of CD44v6 expression promoted by Wnt pathway.

PI3K Inhibition Reduces CD44v6 Expression and Metastasis Formation in CRC

To investigate the signaling pathways involved in the metastatic behavior of CR-CSCs, we analyzed the posttranslational modifications of the proteins commonly related to the metastatic signaling pathways. Immunoblot analysis revealed a significant downregulation of PTEN and a considerable upregulation of phosphatidylinositol 3-kinase (PI3K) and activation of AKT in CRC sphere cells treated with HGF, OPN, and SDF-1, whereas a constitutive activation of the PI3K/AKT pathway was observed in CD44v6$^+$ cells (Figures 6A, 6B, and S6A). Inhibition

(D) Kinetics of in vivo whole-body imaging analysis of metastasis formation at the indicated time following spleen injection of CD44v6$^+$ and CD44v6$^-$ sphere cells, untreated and treated with CAF-CM for 24 hr.

(E) Size of primary (8 weeks) and secondary (6 weeks) subcutaneous tumors generated by injection of magnetically sorted CD44v6$^+$ and CD44v6$^-$ sphere cells, alone and together with CAF. Data are expressed as mean ± SD of four independent experiments, performed with cells from different patients. Inset, representative Azan-Mallory analysis in CD44v6$^+$ and CD44v6$^-$ tumor xenografts. The scale bars represent 100 μm.

(F) HGF, OPN, SDF, and TGF-β production in CAFs, spheres, and CD44v6$^+$ and CD44v6$^-$ cells. Data are mean ± SD of four independent experiments using cells from different patients. Whiskers: Vmin, Vmax (log10).

(G) mRNA expression levels of *HGF*, *OPN*, *TGF-β*, and *SDF* on freshly sorted CD45$^-$/EpCAM$^-$/CD90$^+$, CD45$^-$/EpCAM$^+$/CD90$^-$/CD44v6$^+$, and CD45$^-$/EpCAM$^+$/CD90$^-$/CD44v6$^-$ cells from colon cancer specimens. *GAPDH* was used as housekeeping control gene. Data are expressed as mean ± SD of five independent experiments performed with cells from different patients.

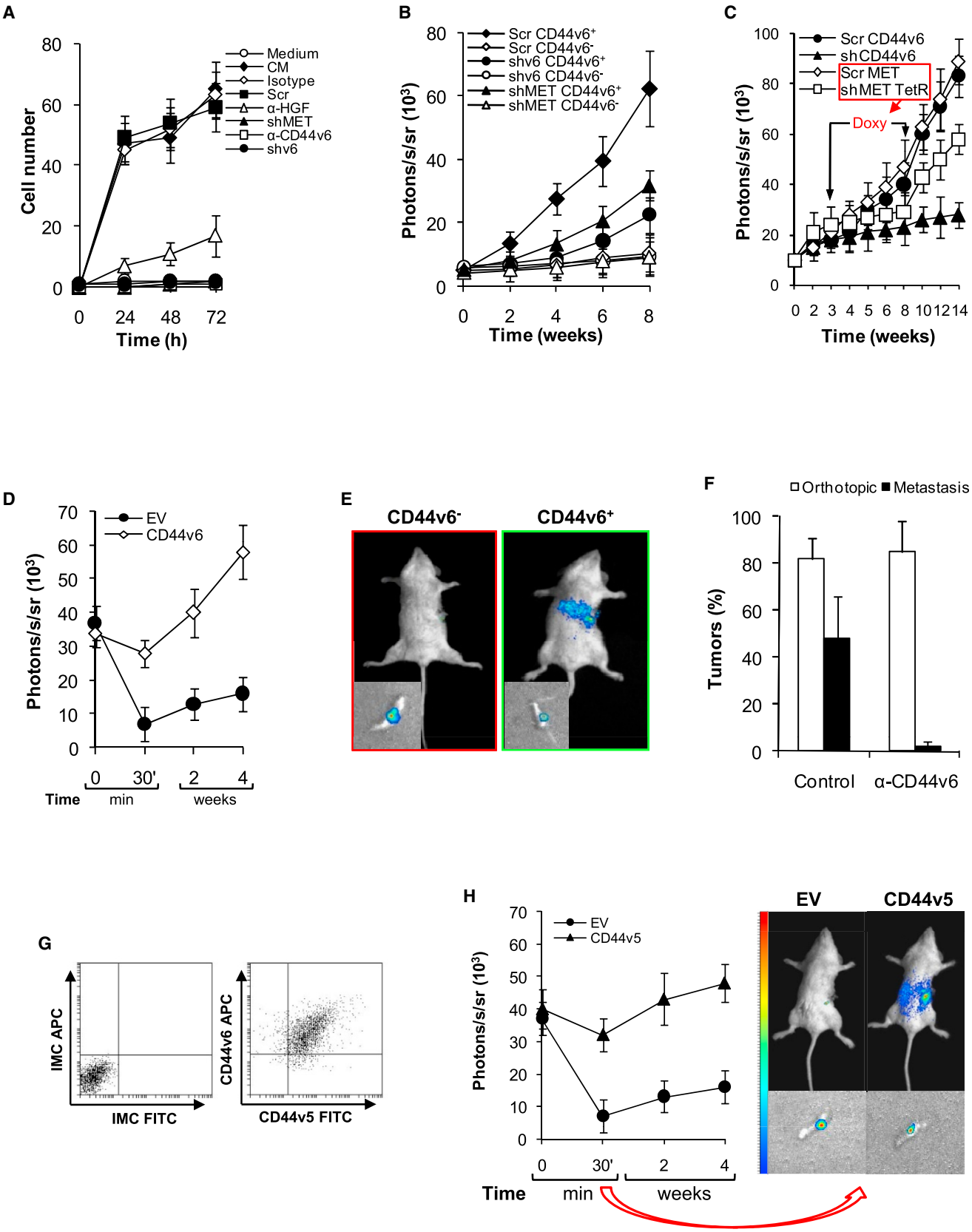

(legend on next page)

of PI3K/AKT pathway in CRC spheres caused a significant reduction of cell viability, particularly in samples bearing PI3K mutation (Figure S6B), and hampered the expression of CD44v6 induced by HGF, OPN, and SDF-1 on CD44v6$^-$ cells (Figures 6C and S6C). Of note, CD44v6$^+$ cells were the major subset dying in vitro after PI3K inhibition (Figure 6D). Moreover, the analysis of early signaling showed that BMP4 upregulated the expression of PTEN and impaired the activation of the PI3K/AKT pathway promoted by HGF, OPN, and SDF-1 (Figures 6E and S6D). To investigate whether the dependence of CD44v6$^+$ cells to the PI3K/AKT pathway may be exploited to prevent or reduce metastasis formation in CRC, we determined the effect of treatment with the PI3K inhibitor BKM120 on the orthotopic preclinical model. Such treatment considerably reduced the metastatic spreading of CRC cells, regardless of the presence of *PI3K*-activating mutations (Figures 6F and S6E). Accordingly, exogenous expression of PI3K re-established the expression of CD44v6 and the in vivo migration of CD44v6$^-$ cells (Figures S6F–S6H), confirming that the PI3K pathway plays a major role in promoting the metastatic activity of CRC cells.

CD44v6 Expression Is a Biomarker for the Clinical Outcome of CRC Patients

We next explored the clinical relevance of CD44v6 as a prognostic biomarker. In line with a meta-analysis of 511 patients proposing a correlation between detection of CD44v6 and worse overall survival (Fan et al., 2012; Saito et al., 2013), the analysis of a large cohort of primary and metastatic CRCs showed a significant negative correlation between CD44v6 expression and survival probability of CRC patients (Figures 7A–7D). This correlation was not detectable in patients with stage I and II, most likely because a higher number of patients and a longer followup would be required to detect differences in low-stage tumors (Figure S7A). Of note, multivariate analysis indicated that CD44v6 is an independent negative prognostic factor in both cohorts of patients (Figure S7B).

Given that HGF, OPN, and SDF-1 induce the expression of CD44v6 in immature CRC cells, we investigated the possible correlation of these cytokines with the presence of CD44v6 in tumor specimens from CRC patients. The analysis of ten patients showed that HGF, OPN, and SDF-1 are present at higher levels in tumors with increased number of CD44v6$^+$ cells as compared with tumors with fewer or no CD44v6$^+$ cells (Figure S7C), suggesting that the three cytokines contribute to increase the number of CD44v6$^+$ cells in tumors of CRC patients.

DISCUSSION

Here, we demonstrated that CR-CSCs express CD44v6, which is a functional marker able to confer the ability to migrate at distant sites and develop CRC metastasis, as confirmed by the significant inverse correlation between patient survival and CD44v6 expression. Several groups have identified tumorigenic populations with stem-like features in CRC (Barker et al., 2007; Dalerba et al., 2007; Huang et al., 2009; O'Brien et al., 2007; Ricci-Vitiani et al., 2007; Todaro et al., 2007; Vermeulen et al., 2008, 2010). These cells are able to promote tumor growth and are regarded as an ideal cell target to obtain effective therapies. However, the growth of primary tumors is usually not life-threatening, unlike the occurrence of metastatic lesions (Valastyan and Weinberg, 2011). Because MET is widely expressed in CRC (Takeuchi et al., 2003), the concomitant expression of CD44v6 and MET in all CR-CSCs empowers these cells to form metastasis and severely affect patient prognosis (Minoo et al., 2010; Peng et al., 2008).

EMT is exploited by cancer cells to increase self-renewal and migration through a process that favors the emergence of CSCs (Mani et al., 2008). We show that CD44v6$^+$ CRC cells display β-catenin activation and EMT traits coupled with a considerable migratory activity, which explains the metastatic features of immunocompromised mice treated with these cells. Our data reveal that the EMT and metastatic potential of CR-CSCs is increased by microenvironmental signals promoting the expression of CD44v6. HGF, SDF-1, and OPN are potent inducers of CD44v6 and provide metastatic activity to tumorigenic cells. Targeting MET or CD44v6 completely prevented the invasive capability of the tumorigenic CRC cells, indicating that the metastatic potential depends on signaling generated by HGF via CD44v6 and MET. These receptors cooperate to activate the PI3K/AKT pathway, which promotes migration and survival signaling in

Figure 4. Inhibition of CD44v6 and MET Hampers the Metastatic Potential of CR-CSCs

(A) Invasion assay of sphere cells untreated (medium) and treated with α-CD44v6 or transduced with control shRNA (Scr), *MET* shRNA (shMET), or *CD44v6* shRNA (shCD44v6). α-HGF was added to the lower part of transwell containing NIH 3T3-CM (CM). Data are mean ± SD of six independent experiments using cells from different patients.

(B) In vivo whole-body imaging analysis of orthotopic xenografts and metastasis growth at the indicated weeks generated by 5 × 10^3 sphere cells transduced with scramble CD44v6$^+$ (Scr CD44v6$^+$), scramble CD44v6$^-$ (Scr CD44v6$^-$), shCD44v6 CD44v6$^+$ (shv6 CD44v6$^+$), shCD44v6 CD44v6$^-$ (shv6 CD44v6$^-$), shMET CD44v6$^+$, or shMET CD44v6$^-$. Data are expressed as mean ± SD of five independent experiments.

(C) Kinetics of in vivo whole-body imaging analysis of orthotopic xenografts and metastasis growth at the indicated weeks generated by 5 × 10^3 sphere cells transduced with Scr CD44v6, shCD44v6, Scr MET, or doxycycline-inducible shMET (shMET TetR). Data are expressed as mean ± SD of three independent experiments.

(D) Kinetics of in vivo imaging analysis of metastatic formation induced by injection of CD44v6$^-$ CRC sphere cells transduced with empty vector (EV) and *CD44v6* synthetic gene, at the indicated time points after splenectomy.

(E) In vivo imaging analysis of syngeneic BALB/c mice obtained by spleen injection of enriched CD44v6$^+$ and CD44v6$^-$ colon-26 cells, 30 min after splenectomy.

(F) Growth percentage of primary tumors and corresponding liver metastasis sustained by parental cancer cells treated with isotype-matched control (IMC) and neutralizing antibody against CD44v6 (α-CD44v6). Data are mean ± SD of results obtained from 12 independent experiments performed with cells of four different patients.

(G) Flow cytometry profiles of CD44v5/CD44v6 in CD44v6$^+$ CRC cells. Data are representative of four independent experiments using cells from different patients.

(H) Kinetics of in vivo imaging analysis of metastatic colony formation induced by injection of CD44v6$^-$ CRC sphere cells transduced with LUC-GFP EV and *CD44v5* synthetic gene, at the indicated time points after splenectomy (left panel). In vivo whole-body imaging analysis of migrating cells transduced with LUC-GFP EV and *CD44v5* synthetic gene generated 30 min after splenectomy (right panels).

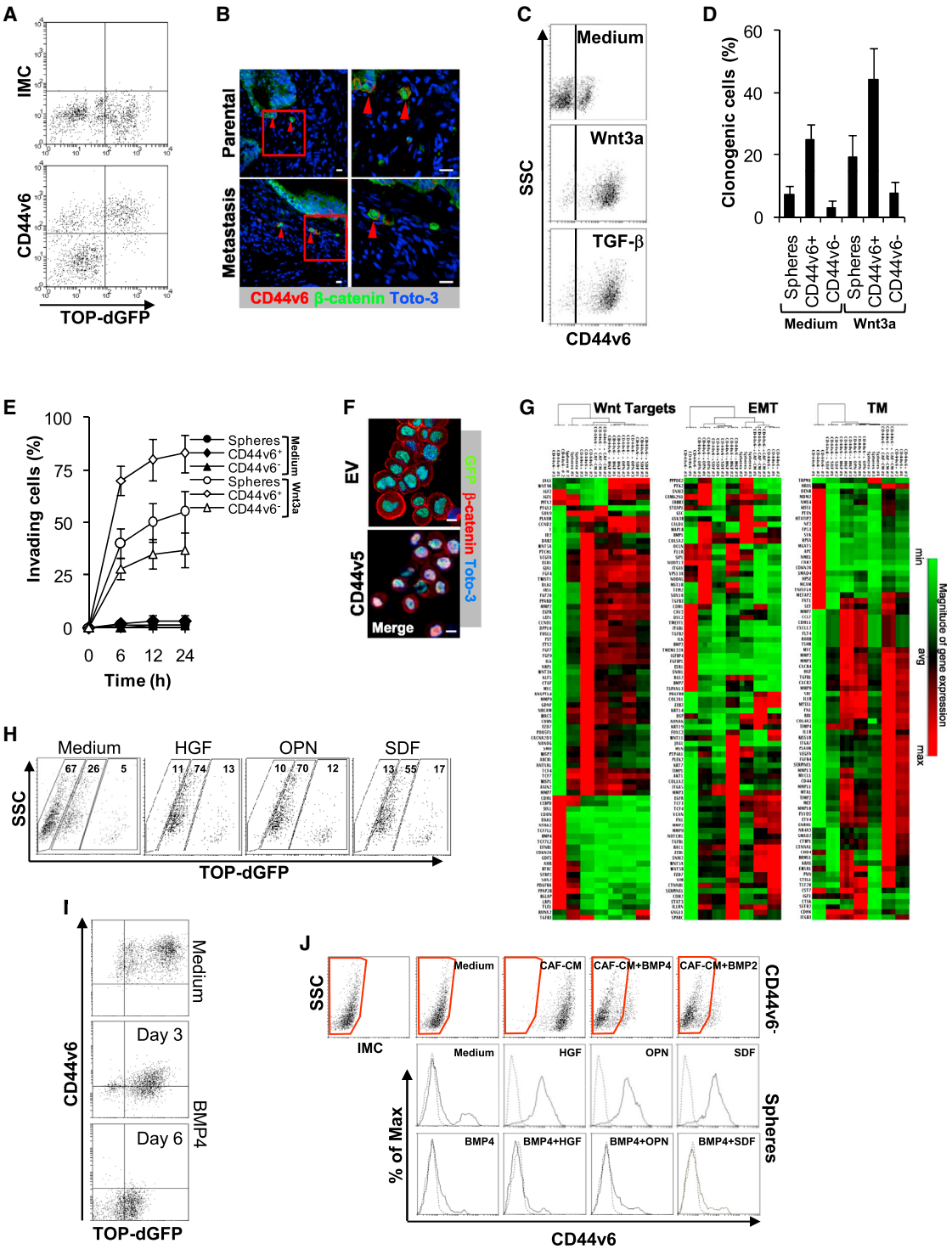

Figure 5. CD44v6 Expression Is Critically Regulated by the Wnt Pathway

(A) Flow cytometry analysis of IMC and CD44v6 on colon cancer sphere cells transduced with TOP-destabilized GFP (dGFP).

(B) Expression of CD44v6 (red color) and β-catenin (green color) on paraffin-embedded sections of parental CRC and its liver metastasis tissue at the front of invasion. Nuclei were counterstained with Toto-3 (blue color). The scale bars represent 20 μm.

(C) Clonogenic assay of spheres and CD44v6$^+$ and CD44v6$^-$ enriched cells cultured in presence of CAF-CM or treated with Wnt3a.

(D) Migration assay of bulk (spheres) and CD44v6$^+$ and CD44v6$^-$ sphere cells untreated (medium) and pretreated with Wnt3a for 6 hr.

(E) Flow cytometry analysis of CD44v6 on sphere cells untreated and treated with Wnt3a or TGF-β. Data are representative of three independent experiments.

(F) Immunofluorescence analysis of β-catenin (red color) and GFP on CD44v6$^-$ CRC sphere cells transduced with LUC-GFP EV and *CD44v5* synthetic gene (green color). Nuclei were stained with Toto-3 (blue color). The scale bars represent 10 μm.

(legend continued on next page)

CR-CSCs. Activation of Wnt signaling plays a key role in maintaining the stem cell pool in the gut and promoting self-renewal of CR-CSCs (de Lau et al., 2011; Leedham et al., 2013; Ootani et al., 2009; van Es et al., 2012). Cytokines released in the microenvironment contribute significantly to maintain the undifferentiated status and clonogenic activity of the tumorigenic cells (Bissell and Labarge, 2005; Medema and Vermeulen, 2011; Vermeulen et al., 2010). Our data indicate that this property is not confined to HGF (Vermeulen et al., 2010), but it is shared by OPN and SDF-1, which enhance β-catenin activation in CR-CSCs. A similar effect may be mediated by TGF-β, which is produced by both CAFs and CD44v6$^+$ cells. Whereas CAFs seem to play a key role in the induction of CD44v6, it is likely that autocrine production of OPN and TGF-β may contribute to promote the metastatic activity of CD44v6$^+$ cells. The inability of all these cytokines to induce the expression of CD44v6 on more-differentiated CRC cells may be related to the low activation of β-catenin observed in these cells, despite the presence of genomic alterations that should provide a constitutive activation of the Wnt pathway. Thus, CD44v6 expression appears as part of a more complex system that confers self-renewal and metastatic properties to CR-CSCs. Targeting CD44v6 expression prevented metastasis formation without affecting the growth of primary tumors. Likewise, delivery of CD44v6 in negative cells restores migration and in vivo colonization, without providing self-renewal properties to target cells.

We recently demonstrated that BMP4 counteracts Wnt activity in CR-CSCs and promotes their differentiation via upregulation of PTEN and inhibition of PI3K (Lombardo et al., 2011), which maintain the undifferentiated status of the tumorigenic population (Vermeulen et al., 2008). CD44v6$^+$ cells show enhanced activation of the PI3K/AKT pathway, which is triggered by ligand binding and by the epigenetic silencing of PTEN that characterized CR-CSCs (Lombardo et al., 2011; Ricci-Vitiani et al., 2010). PI3K promotes the expression of CD44v6 in CRC progenitors, whereas its inhibition impairs migration and survival of CD44v6$^+$ CRC cells, which are significantly more sensitive to PI3K inhibition than the CD44v6$^-$ counterpart. Because clinical trials with available drugs targeting PI3K or HGF pathways have not been designed in the adjuvant setting, these findings may have considerable therapeutic implications (Ghiso and Giordano, 2013; Rodon et al., 2013).

Although some CD44v6$^-$ cells could be tumorigenic and develop small tumors, most tumorigenic activity seems to be confined in the CD44v6$^+$ population, which contains virtually all the cells with high β-catenin activation. Because there is a significant overlap between tumorigenic and metastagenic cells, it is likely that the relative density of CSCs in CRC directly correlates with the metastatic propensity of tumor lesions. In this context, CD44v6 appears as a key functional biomarker critically involved in the main features of cancer progression.

EXPERIMENTAL PROCEDURES

Five-week-old nonobese diabetic/severe combined immunodeficiency mice from Charles River Laboratories were maintained in accordance to the institutional guidelines of the University of Palermo Animal Care Committee.

Tissue Collection an Isolation and Culture of Cancer Cells

Colorectal cancer tissues were obtained at the time of resection from 36 patients (age range 52–78 years) and liver metastasis from 18 matched patients, in accordance with the ethical standards of the Institutional Committee on Human Experimentation (see Table S1). Normal colon mucosa was obtained from the histologically uninvolved resection.

Sphere purification and sphere-derived adherent cultures (SDACs) were obtained as previously described (Lombardo et al., 2011; Todaro et al., 2007).

Primary fibroblasts were isolated from colorectal cancer tissues, cultured in presence of 10% FBS Dulbecco's modified Eagle's medium in adherent conditions, and indicated as CAFs. Murine colon carcinoma cells (colon-26) were cultured in medium supplemented with 2 mM L-glutamine and 10% FBS in adherent conditions (CLS Cell Lines Service).

Flow Cytometry and Magnetic Sorting

Cells, where indicated, were stained with primary conjugated EpCAM-PerCP–Cy5.5 (EBA-1; mouse immunoglobulin G_1 [IgG_1]; BD Biosciences), CD44v6-antigen-presenting cell (APC) (2F10; mouse IgG_1; R&D Systems), MET-fluorescein isothiocyanate (FITC) (95106; mouse IgG_1; R&D Systems), CD44v5 (3D2; mouse IgG_1; R&D Systems) antibodies, or corresponding isotype-matched controls. Magnetic cell separation was performed on cells stained with CD44v6 (VFF-7; mouse IgG1; Abcam) rinsed and incubated with microbeads (130-047 102 anti-mouse IgG_1 microBeads; Miltenyi Biotec). Quality of sorting was monitored by flow cytometry with specific antibody for CD44v6-APC. Freshly purified CRC cells were stained for CD45-PerCP-Cy5.5 (TU116; mouse IgG_{1k}; BD Biosciences), CD90-FITC (5E10; mouse IgG_{1k}; BD Biosciences), EpCAM-phycoerythrin (BD Biosciences), and CD44v6-APC; sorted; and collected in TRIzol for reverse transcriptase analysis. In order to analyze changes of CD44v6 expression, flow cytometry analyses were assessed on cells treated with HGF (100 ng/ml), OPN (1 μg/ml), SDF (100 ng/ml), 10% FBS, CAF-CM, transforming growth factor-beta1 (recombinant human TGF-β1; 4 ng/ml; Peprotech), and BKM120. Cells were also pre- or posttreated with BMP2 or BMP4 (100 ng/ml; R&D Systems) up to 6 days.

Immunofluorescence/Immunohistochemistry

Cells were fixed and permeabilized as previously reported (Todaro et al., 2007) and exposed overnight at 4°C to antibodies against CD133 (AC133; mouse IgG_1; Miltenyi Biotec), MET (c-28; rabbit IgG; Santa Cruz Biotechnology), CD44v6 (2F10; mouse IgG1; R&D Systems), β-catenin (H102; rabbit IgG; Santa Cruz Biotechnology), or isotype-matched controls. Then, cells were labeled with secondary antibodies (Invitrogen). Nuclei counterstaining was performed using Toto-3 iodide.

Tissue microarrays (TMAs) slides were exposed to specific antibodies against CD44v6, examined microscopically by three independent observers blinded to clinicopathological information, and stratified according to the CD44v6 expression.

Invasion Assay

Cells (1.5×10^3), untreated and treated with hepatocyte growth factor (recombinant human HGF; 100 ng/ml; Peprotech), osteopontin (OPN; 1 μg/ml; Sigma), stromal-cell-derived factor-1α (recombinant human SDF-1α; 100 ng/ml; Peprotech), CAF-CM, neutralizing antibody against CD44v6 (15 μg/ml; 2F10; mouse IgG_1; R&D Systems), isotype-matched control (15 μg/ml; human

(G) Clustergrams of up- and downregulated Wnt targets and epithelial-mesenchymal transition (EMT)- and tumor metastasis (TM)-related genes in spheres and CD44v6$^+$ and CD44v6$^-$ cells, untreated and treated with HGF, OPN, SDF, and CAF-CM for 24 hr. Gene expression profiles are derived from cells purified from three different patients.
(H) Flow cytometry analysis of TOP-dGFP in CD44v6-depleted CRC sphere cells untreated (medium) or treated with HGF, OPN, and SDF. SSC, side scatter.
(I) Flow cytometry analysis of CD44v6 in TOP-dGFP transduced CD44v6$^+$ cells untreated (medium) or treated with BMP4 up to 6 days.
(J) Flow cytometry profiles of representative IMC and CD44v6 in CD44v6$^-$ sphere cells cultured with medium or CAF-CM and posttreated with BMP4 or BMP2 for 48 hr (upper panels) and in CRC sphere cells untreated (medium) or treated with BMP4 with or without HGF, OPN, and SDF (lower panels).

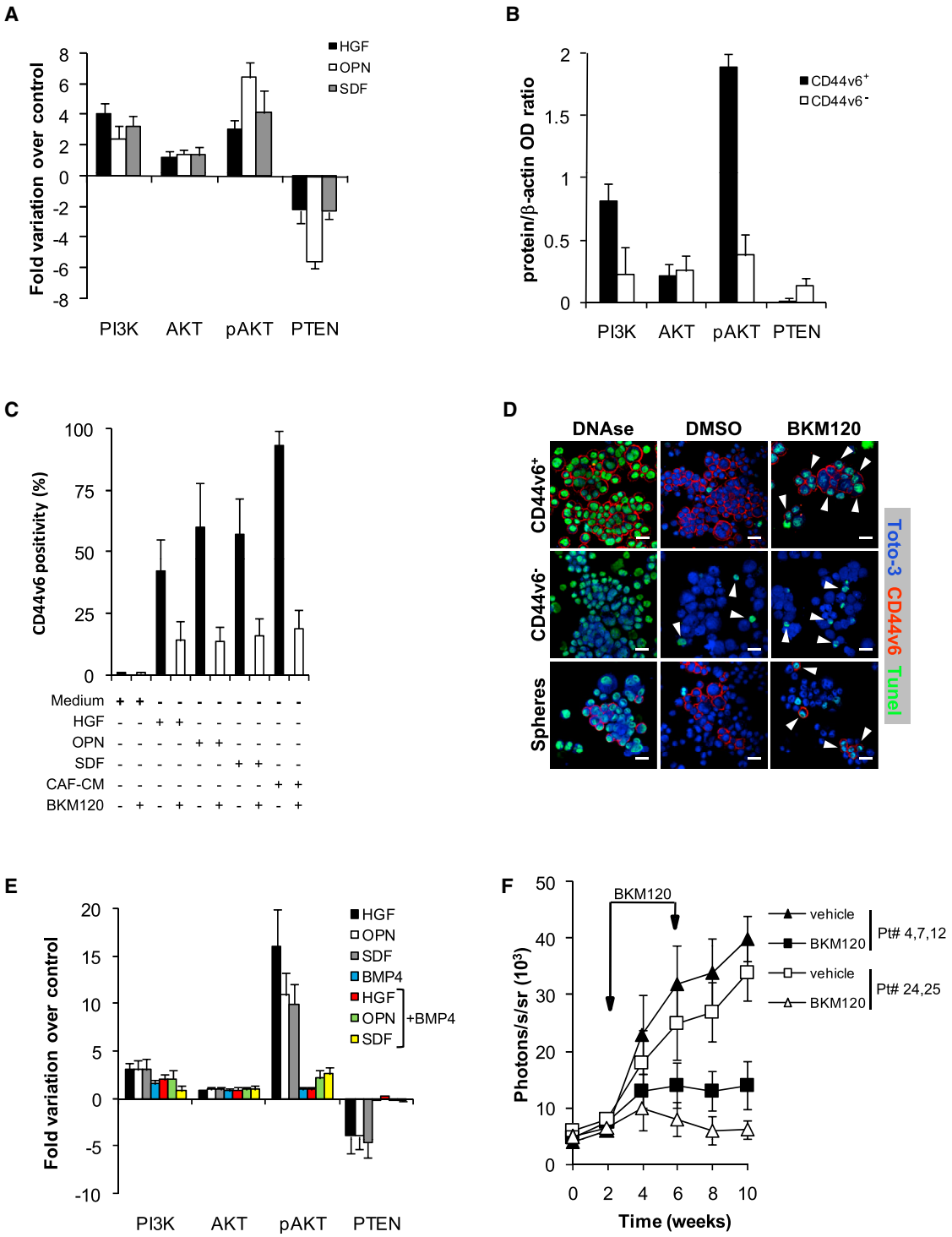

Figure 6. PI3K Inhibition Promotes Death of CD44v6 Cell Fraction

(A) Fold protein level changes of PI3K, AKT, phosho-AKT (pAKT), and PTEN in eight different sphere cell lines untreated and treated with HGF, OPN, and SDF for 24 hr.

(B) Relative protein expression levels of PI3K, AKT, pAKT, and PTEN on CD44v6$^+$ and CD44v6$^-$ sphere cells. Data are mean ± SD of five independent experiments performed using different cell lines. OD, optical density.

(C) CD44v6 expression in CD44v6$^-$ sphere cells untreated (medium) and treated with HGF, OPN, SDF, and CAF-CM, alone or in combination with BKM120 for 48 hr. Data are expressed as mean ± SD of six independent experiments.

(D) Confocal microscopy analysis of apoptotic events on cytospun disaggregated spheres and CD44v6$^+$ and CD44v6$^-$ cells treated with DMSO or 1 μM BKM120 and stained for CD44v6 (red color) and TUNEL (green color, white arrows). Nuclei were counterstained by Toto-3 (blue color). Positive control was assessed with DNase pretreated cells. The scale bars represent 20 μm.

(legend continued on next page)

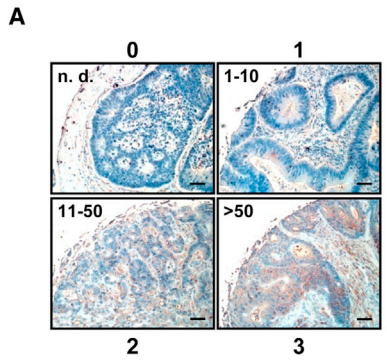

B

TMA *(Tri)*

Stage	Pts	CD44v6 Score 2/3 (%)
I-II	77	14 (18.2)
III-IV	200	63 (31.5)
Pearson's Chi Square test: p=0.03		

TMA *(NIH)*

Stage	Pts	CD44v6 Score 2/3 (%)
I-II	71	10 (14.1)
III-IV	89	47 (59.8)
Pearson's Chi Square test: p<0.0001		

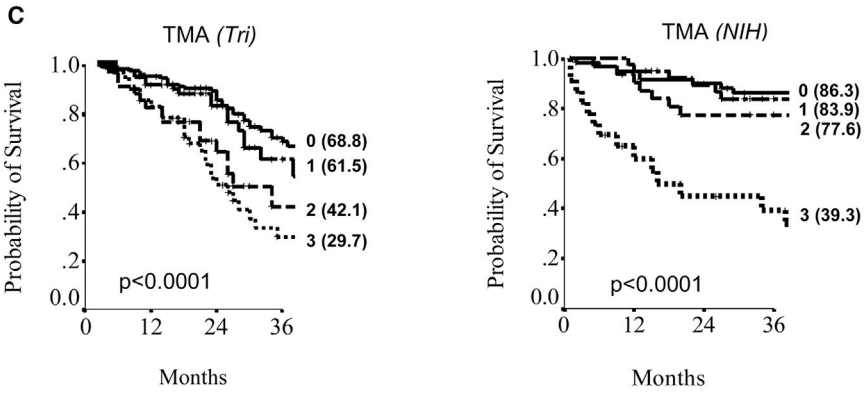

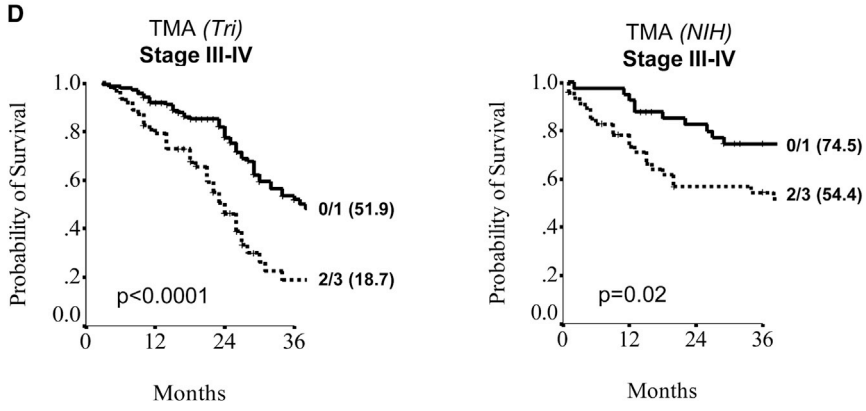

Figure 7. CD44v6 Expression Correlates with Poorer Prognosis

(A) Representative immunohistochemical analysis of CD44v6 on CRC cores in no detectable (0), up to ten positive cells (1), 11–50 positive cells (2), and over 50 positive cells (3). The scale bars represent 50 μm. n.d., no detectable.

(B) Association of CD44v6 expression with score 2/3 and the pathological staging in CRC patients included in the TMAs provided by TRISTAR technology group (Tri) and National Institutes of Health (NIH).

(C) Kaplan-Meier survival curves based on CD44v6 expression, according to (A), in all patients analyzed in Tri and NIH TMAs.

(D) Kaplan-Meier survival curves according to CD44v6 expression (0/1 and 2/3) as in (A) analyzed in patients with stages III to IV.

CD3ε; UCHT1; mouse IgG_1; R&D Systems), Wnt3a (150 ng/ml; R&D Systems) or transduced with control shRNA (Scr), MET shRNA (shMET), or CD44v6 shRNA (shv6), were plated into Matrigel-coated (BD Biosciences) transwell of 8 μm pore size (Corning Life Sciences). Supernatant of National Institutes of Health (NIH) 3T3 cells cultured in stem cell medium (SCM) (CM) or SCM alone (medium) or supplemented with cytokines were used as chemoattractant in the transwell lower part. Antibodies against HGF (10 μg/ml; 24612; mouse IgG_1; R&D Systems) and OPN (5 μg/ml; AF1433; goat IgG; R&D Systems) were mixed with conditioned medium and placed in the lower part of transwell. AMD3100 (50 μM; Sigma-Aldrich) was added to sphere cells for 90 min and replaced every 6 hr up to 72 hr in the upper part of the transwell. Migration was observed and counted microscopically up to 72 hr.

Clonogenic Assay

Cells were plated in presence of stem cell medium, CAF-CM or Wnt3a, replaced every 5 days, on ultra-low-adhesion 96-well plates at a concentration of a single cell per well. Wells containing either none or more than one cell were excluded for the analysis.

Animals and Orthotopic Tumor Model

Orthotopic xenografts were obtained using either 5×10^3 or 15×10^3 CRC sphere cells or freshly purified parental cancer cells $CD44v6^+$- and $CD44v6^-$-enriched cells. Intrasplenic injection of 3×10^5 luciferase (LUC)/GFP-transduced $CD44v6^+$ and $CD44v6^-$ cells, untreated and treated with CAF-CM for 24 hr, or $CD44v6^-$ cells overexpressing CD44v6 or CD44v5 was performed to evaluate the metastatic potential. Subcutaneous xenografts were obtained by the injection of enriched $CD44v6^+$ and $CD44v6^-$ cells, alone or in combination with CAF (2.5×10^3 cells; ratio 1:1). Secondary tumors were generated by the inoculation of 5×10^3 primary bulk xenograft cells. In the syngeneic model, 3×10^5 $CD44v6^+$ and $CD44v6^-$ colon-26 cells transduced with LUC/GFP were injected into the spleen of BALB/c-mice.

Cytokines Quantification

Quantification for HGF, OPN, SDF-1, and TGF−β production was assessed by using multiplex Bio-Plex Pro Assays (Bio-Rad; Human Cancer Biomarker

(E) Fold change of PI3K, AKT, pAKT, and PTEN in $CD44v6^-$ sphere cells untreated and treated with HGF, OPN, and SDF for 24 hr, alone or in combination with BMP4 for additional 24 hr.

(F) In vivo imaging analysis of orthotopic tumor and liver metastasis growth at the indicated weeks generated by CRC sphere cells treated with PBS (vehicle) and BKM120. Data are representative of four independent experiments.

Panel 1-4 No. 171-AC500M; Human Cytokine SDF-1α Set No. 171-B6019M; TGF-β 3-plex Assay No. 171-W4001M). Raw data (mean fluorescent intensity) from all kits were analyzed by Bio-Plex Software (Bio-Rad).

Real-Time PCR

Quantitative real-time PCR analysis was performed in a master mix containing the following primer sets: Hs00300159_m1 (*HGF*), Hs00959010_m1 (*OPN*), Hs00998133_m1 (*TGF-β1*), Hs00171022_m1 (*SDF-1*), and Hu-GAPDH (Applied Biosystems). Data processing and statistical analysis were performed using the ABI PRISM SDS software v2.1 (Applied Biosystems).

The RT^2 Profiler PCR array was assessed for genes related to Wnt targets, EMT, and tumor metastasis (TM) (PAHS-243ZR-12, PAHS-090ZR, PAHS-028ZR-12; SuperArray Bioscience). Cycle threshold values were calculated for all the genes present on the array and normalized using the average of five housekeeping genes (*ACTB*, *B2M*, *HPRT1*, *RPLP0*, and *GAPDH*). RT^2 Profiler PCR array data analysis was represented by clustergrams based on Pearson's correlation of $2^{\wedge}(\Delta Ct)$.

Statistical Analysis

Data were expressed as mean ± SD. Statistical significance was determined by ANOVA (one-way or two-way) with Bonferroni posttest.

For TMA analysis, associations between categorical variables were tested by the Pearson Chi-Square test, Fisher Exact tests, or Chi square for trend, when appropriate. The receiver-operating characteristic curve analysis was used in order to find possible optimal cutoffs of the CD44v6 capable of splitting patients into groups with different outcomes probabilities. Kaplan-Meier method was used to estimate survival curves, whereas differences between subgroups were assessed by the log rank test. All significance was defined at the $p < 0.05$ level.

SUPPLEMENTAL INFORMATION

Supplemental Information for this article includes Supplemental Experimental Procedures, seven figures, and one table and can be found with this article online at http://dx.doi.org/10.1016/j.stem.2014.01.009.

AUTHOR CONTRIBUTIONS

M.T., M.G., V.C., and F.I. conducted the experiments; A.B., S.V., and M.T. assessed the in vivo experiments and analyzed the tissue microarrays according to histopathological criteria. M.B. and T.A. performed the flow cytometry analysis. I.S. analyzed the tissue microarray data and executed statistical analysis. G.C. and G.G. provided colon cancer specimens. F.D. supplied scientific suggestions and critical review. R.D.M. and G.S. wrote the manuscript, planned and supervised the experiments, and interpreted the data.

ACKNOWLEDGMENTS

We thank Francesco Calò for graphic images help, Alessandro Gorgone and Giovanni Tomaselli for technical assistance, and Alessandro Scopelliti for immunohistochemical analyses and critical comments. This work was funded by AIRC 5x1000 (9979) to G.S. and R.D.M. M.G. is a FIRC fellowship recipient.

Received: November 1, 2012
Revised: October 22, 2013
Accepted: January 14, 2014
Published: March 6, 2014

REFERENCES

Al-Hajj, M., Wicha, M.S., Benito-Hernandez, A., Morrison, S.J., and Clarke, M.F. (2003). Prospective identification of tumorigenic breast cancer cells. Proc. Natl. Acad. Sci. USA *100*, 3983–3988.

Barker, N., van Es, J.H., Kuipers, J., Kujala, P., van den Born, M., Cozijnsen, M., Haegebarth, A., Korving, J., Begthel, H., Peters, P.J., and Clevers, H. (2007). Identification of stem cells in small intestine and colon by marker gene Lgr5. Nature *449*, 1003–1007.

Bissell, M.J., and Labarge, M.A. (2005). Context, tissue plasticity, and cancer: are tumor stem cells also regulated by the microenvironment? Cancer Cell *7*, 17–23.

Brabletz, T., Jung, A., Spaderna, S., Hlubek, F., and Kirchner, T. (2005). Opinion: migrating cancer stem cells - an integrated concept of malignant tumour progression. Nat. Rev. Cancer *5*, 744–749.

Cantor, H., and Shinohara, M.L. (2009). Regulation of T-helper-cell lineage development by osteopontin: the inside story. Nat. Rev. Immunol. *9*, 137–141.

Chaffer, C.L., and Weinberg, R.A. (2011). A perspective on cancer cell metastasis. Science *331*, 1559–1564.

Dalerba, P., Dylla, S.J., Park, I.K., Liu, R., Wang, X., Cho, R.W., Hoey, T., Gurney, A., Huang, E.H., Simeone, D.M., et al. (2007). Phenotypic characterization of human colorectal cancer stem cells. Proc. Natl. Acad. Sci. USA *104*, 10158–10163.

de Lau, W., Barker, N., Low, T.Y., Koo, B.K., Li, V.S., Teunissen, H., Kujala, P., Haegebarth, A., Peters, P.J., van de Wetering, M., et al. (2011). Lgr5 homologues associate with Wnt receptors and mediate R-spondin signalling. Nature *476*, 293–297.

Di Renzo, M.F., Olivero, M., Giacomini, A., Porte, H., Chastre, E., Mirossay, L., Nordlinger, B., Bretti, S., Bottardi, S., Giordano, S., et al. (1995). Overexpression and amplification of the met/HGF receptor gene during the progression of colorectal cancer. Clin. Cancer Res. *1*, 147–154.

Fan, C.W., Wen, L., Qiang, Z.D., Chen, T., Zhou, Z.G., Mo, X.M., and Hu, J.K. (2012). Prognostic significance of relevant markers of cancer stem cells in colorectal cancer - a meta analysis. Hepatogastroenterology *59*, 1421–1427.

Ghiso, E., and Giordano, S. (2013). Targeting MET: why, where and how? Curr. Opin. Pharmacol. *13*, 511–518.

Hanahan, D., and Coussens, L.M. (2012). Accessories to the crime: functions of cells recruited to the tumor microenvironment. Cancer Cell *21*, 309–322.

Hardwick, J.C., Van Den Brink, G.R., Bleuming, S.A., Ballester, I., Van Den Brande, J.M., Keller, J.J., Offerhaus, G.J., Van Deventer, S.J., and Peppelenbosch, M.P. (2004). Bone morphogenetic protein 2 is expressed by, and acts upon, mature epithelial cells in the colon. Gastroenterology *126*, 111–121.

Hermann, P.C., Huber, S.L., Herrler, T., Aicher, A., Ellwart, J.W., Guba, M., Bruns, C.J., and Heeschen, C. (2007). Distinct populations of cancer stem cells determine tumor growth and metastatic activity in human pancreatic cancer. Cell Stem Cell *1*, 313–323.

Huang, E.H., Hynes, M.J., Zhang, T., Ginestier, C., Dontu, G., Appelman, H., Fields, J.Z., Wicha, M.S., and Boman, B.M. (2009). Aldehyde dehydrogenase 1 is a marker for normal and malignant human colonic stem cells (SC) and tracks SC overpopulation during colon tumorigenesis. Cancer Res. *69*, 3382–3389.

Jemal, A., Bray, F., Center, M.M., Ferlay, J., Ward, E., and Forman, D. (2011). Global cancer statistics. CA Cancer J. Clin. *61*, 69–90.

Lee, C.J., Dosch, J., and Simeone, D.M. (2008). Pancreatic cancer stem cells. J. Clin. Oncol. *26*, 2806–2812.

Leedham, S.J., Rodenas-Cuadrado, P., Howarth, K., Lewis, A., Mallappa, S., Segditsas, S., Davis, H., Jeffery, R., Rodriguez-Justo, M., Keshav, S., et al. (2013). A basal gradient of Wnt and stem-cell number influences regional tumour distribution in human and mouse intestinal tracts. Gut *62*, 83–93.

Lombardo, Y., Scopelliti, A., Cammareri, P., Todaro, M., Iovino, F., Ricci-Vitiani, L., Gulotta, G., Dieli, F., de Maria, R., and Stassi, G. (2011). Bone morphogenetic protein 4 induces differentiation of colorectal cancer stem cells and increases their response to chemotherapy in mice. Gastroenterology *140*, 297–309.

Mani, S.A., Guo, W., Liao, M.J., Eaton, E.N., Ayyanan, A., Zhou, A.Y., Brooks, M., Reinhard, F., Zhang, C.C., Shipitsin, M., et al. (2008). The epithelial-mesenchymal transition generates cells with properties of stem cells. Cell *133*, 704–715.

Medema, J.P., and Vermeulen, L. (2011). Microenvironmental regulation of stem cells in intestinal homeostasis and cancer. Nature *474*, 318–326.

Minoo, P., Zlobec, I., Peterson, M., Terracciano, L., and Lugli, A. (2010). Characterization of rectal, proximal and distal colon cancers based on clinicopathological, molecular and protein profiles. Int. J. Oncol. *37*, 707–718.

O'Brien, C.A., Pollett, A., Gallinger, S., and Dick, J.E. (2007). A human colon cancer cell capable of initiating tumour growth in immunodeficient mice. Nature *445*, 106–110.

Ootani, A., Li, X., Sangiorgi, E., Ho, Q.T., Ueno, H., Toda, S., Sugihara, H., Fujimoto, K., Weissman, I.L., Capecchi, M.R., and Kuo, C.J. (2009). Sustained in vitro intestinal epithelial culture within a Wnt-dependent stem cell niche. Nat. Med. *15*, 701–706.

Orian-Rousseau, V. (2010). CD44, a therapeutic target for metastasising tumours. Eur. J. Cancer *46*, 1271–1277.

Orian-Rousseau, V., Chen, L., Sleeman, J.P., Herrlich, P., and Ponta, H. (2002). CD44 is required for two consecutive steps in HGF/c-Met signaling. Genes Dev. *16*, 3074–3086.

Pang, R., Law, W.L., Chu, A.C., Poon, J.T., Lam, C.S., Chow, A.K., Ng, L., Cheung, L.W., Lan, X.R., Lan, H.Y., et al. (2010). A subpopulation of CD26+ cancer stem cells with metastatic capacity in human colorectal cancer. Cell Stem Cell *6*, 603–615.

Patrawala, L., Calhoun, T., Schneider-Broussard, R., Li, H., Bhatia, B., Tang, S., Reilly, J.G., Chandra, D., Zhou, J., Claypool, K., et al. (2006). Highly purified CD44+ prostate cancer cells from xenograft human tumors are enriched in tumorigenic and metastatic progenitor cells. Oncogene *25*, 1696–1708.

Peng, J., Lu, J.J., Zhu, J., Xu, Y., Lu, H., Lian, P., Cai, G., and Cai, S. (2008). Prediction of treatment outcome by CD44v6 after total mesorectal excision in locally advanced rectal cancer. Cancer J. *14*, 54–61.

Pries, R., Witrkopf, N., Trenkle, T., Nitsch, S.M., and Wollenberg, B. (2008). Potential stem cell marker CD44 is constitutively expressed in permanent cell lines of head and neck cancer. In Vivo *22*, 89–92.

Rangaswami, H., Bulbule, A., and Kundu, G.C. (2006). Osteopontin: role in cell signaling and cancer progression. Trends Cell Biol. *16*, 79–87.

Ricci-Vitiani, L., Lombardi, D.G., Pilozzi, E., Biffoni, M., Todaro, M., Peschle, C., and De Maria, R. (2007). Identification and expansion of human colon-cancer-initiating cells. Nature *445*, 111–115.

Ricci-Vitiani, L., Mollinari, C., di Martino, S., Biffoni, M., Pilozzi, E., Pagliuca, A., de Stefano, M.C., Circo, R., Merlo, D., De Maria, R., and Garaci, E. (2010). Thymosin beta4 targeting impairs tumorigenic activity of colon cancer stem cells. FASEB J. *24*, 4291–4301.

Rodon, J., Dienstmann, R., Serra, V., and Tabernero, J. (2013). Development of PI3K inhibitors: lessons learned from early clinical trials. Nat. Rev. Clin. Oncol. *10*, 143–153.

Saito, S., Okabe, H., Watanabe, M., Ishimoto, T., Iwatsuki, M., Baba, Y., Tanaka, Y., Kurashige, J., Miyamoto, Y., and Baba, H. (2013). CD44v6 expression is related to mesenchymal phenotype and poor prognosis in patients with colorectal cancer. Oncol. Rep. *29*, 1570–1578.

Schimanski, C.C., Schwald, S., Simiantonaki, N., Jayasinghe, C., Gönner, U., Wilsberg, V., Junginger, T., Berger, M.R., Galle, P.R., and Moehler, M. (2005). Effect of chemokine receptors CXCR4 and CCR7 on the metastatic behavior of human colorectal cancer. Clin. Cancer Res. *11*, 1743–1750.

Takeuchi, H., Bilchik, A., Saha, S., Turner, R., Wiese, D., Tanaka, M., Kuo, C., Wang, H.J., and Hoon, D.S. (2003). c-MET expression level in primary colon cancer: a predictor of tumor invasion and lymph node metastases. Clin. Cancer Res. *9*, 1480–1488.

Todaro, M., Alea, M.P., Di Stefano, A.B., Cammareri, P., Vermeulen, L., Iovino, F., Tripodo, C., Russo, A., Gulotta, G., Medema, J.P., and Stassi, G. (2007). Colon cancer stem cells dictate tumor growth and resist cell death by production of interleukin-4. Cell Stem Cell *1*, 389–402.

Tölg, C., Hofmann, M., Herrlich, P., and Ponta, H. (1993). Splicing choice from ten variant exons establishes CD44 variability. Nucleic Acids Res. *21*, 1225–1229.

Valastyan, S., and Weinberg, R.A. (2011). Tumor metastasis: molecular insights and evolving paradigms. Cell *147*, 275–292.

Valent, P., Bonnet, D., De Maria, R., Lapidot, T., Copland, M., Melo, J.V., Chomienne, C., Ishikawa, F., Schuringa, J.J., Stassi, G., et al. (2012). Cancer stem cell definitions and terminology: the devil is in the details. Nat. Rev. Cancer *12*, 767–775.

van Es, J.H., Haegebarth, A., Kujala, P., Itzkovitz, S., Koo, B.K., Boj, S.F., Korving, J., van den Born, M., van Oudenaarden, A., Robine, S., and Clevers, H. (2012). A critical role for the Wnt effector Tcf4 in adult intestinal homeostatic self-renewal. Mol. Cell. Biol. *32*, 1918–1927.

Vermeulen, L., Todaro, M., de Sousa Mello, F., Sprick, M.R., Kemper, K., Perez Alea, M., Richel, D.J., Stassi, G., and Medema, J.P. (2008). Single-cell cloning of colon cancer stem cells reveals a multi-lineage differentiation capacity. Proc. Natl. Acad. Sci. USA *105*, 13427–13432.

Vermeulen, L., De Sousa E Melo, F., van der Heijden, M., Cameron, K., de Jong, J.H., Borovski, T., Tuynman, J.B., Todaro, M., Merz, C., Rodermond, H., et al. (2010). Wnt activity defines colon cancer stem cells and is regulated by the microenvironment. Nat. Cell Biol. *12*, 468–476.

Whiteside, T.L. (2008). The tumor microenvironment and its role in promoting tumor growth. Oncogene *27*, 5904–5912.

Wielenga, V.J., van der Neut, R., Offerhaus, G.J., and Pals, S.T. (2000). CD44 glycoproteins in colorectal cancer: expression, function, and prognostic value. Adv. Cancer Res. *77*, 169–187.

Zeilstra, J., Joosten, S.P., van Andel, H., Tolg, C., Berns, A., Snoek, M., van de Wetering, M., Spaargaren, M., Clevers, H., and Pals, S.T. (2014). Stem cell CD44v isoforms promote intestinal cancer formation in Apc(min) mice downstream of Wnt signaling. Oncogene *33*, 665–670.

Zhang, S., Balch, C., Chan, M.W., Lai, H.C., Matei, D., Schilder, J.M., Yan, P.S., Huang, T.H., and Nephew, K.P. (2008). Identification and characterization of ovarian cancer-initiating cells from primary human tumors. Cancer Res. *68*, 4311–4320.